Dynamic strain and switchable polarization

A pathway to enhance the oxygen evolution reaction on $InSnO_2N$

Spezzati, Chiara; Lan, Zhenyun; Castelli, Ivano E.

Published in:
Journal of Catalysis

Link to article, DOI:
10.1016/j.jcat.2022.07.021

Publication date:
2022

Document Version
Publisher's PDF, also known as Version of record

Journal of Catalysis 413 (2022) 720–727

Contents lists available at ScienceDirect

Journal of Catalysis

journal homepage: www.elsevier.com/locate/jcat

Dynamic strain and switchable polarization: A pathway to enhance the oxygen evolution reaction on $InSnO_2N$

Chiara Spezzati [a], Zhenyun Lan [b,*], Ivano E. Castelli [a,*]

[a] Department of Energy Conversion and Storage, Technical University of Denmark, Anker Engelundsvej 411, DK-2800 Kgs. Lyngby, Denmark
[b] School of Materials Science and Engineering, Hefei University of Technology, Hefei, Anhui 230009, PR China

ARTICLE INFO

Article history:
Received 20 April 2022
Revised 2 July 2022
Accepted 19 July 2022
Available online 27 July 2022

Keywords:
Strain engineering
Photoferroics
Polarisation switching
OER overpotentials
Electrocatalysis

ABSTRACT

$InSnO_2N$ is a novel promising material for photoelectrochemical water splitting because of its band gap in the visible range and band edges position, which straddle the redox levels of water. Moreover, this material shows a spontaneous polarization, which could give rise to a photoferroic effect, thus enhancing the power-to-hydrogen conversion efficiency. In this work, we investigate, using Density Functional Theory (DFT) calculations, the photo-electrochemical response of this material to strain. Strain can reduce the reaction overpotentials for the Oxygen Evolution Reaction (OER) to 0.45 V for a −2.5 % compressive strain on the positively polarized material and to 0.40 V for a 2.3 % tensile strain on the negatively polarized structure. When a polarization switching is combined with a dynamic change of the strain during the reaction, the OER overpotential reaches the lowest value of 0.05 V (far below the ideal case for oxides, which is 0.37 V, and what can be reached by considering only the polarization switching at a fixed strain value). This study demonstrates the potential of $InSnO_2N$ as a catalyst for OER and highlights how surface engineering and dynamic catalysis can enhance the electro-catalytic properties of a material.

1. Introduction

Photo-electrochemical water splitting is a promising process to produce clean hydrogen directly from solar energy. The electrons and holes generated through the photovoltaic effect participate in the hydrogen evolution reaction (HER) and oxygen evolution reaction (OER) respectively. The latter is considered the bottleneck of the whole reaction, as it is a four-electrons process against the two-electrons one of HER. The energy requirement for each step of the OER needs to be minimized to achieve high reaction efficiencies. These are affected by the interaction between catalyst and adsorbate and are limited by the Sabatier's principle: a weak interaction leads to a reaction limited by the activation of the reactant, while a strong one to a reaction limited by the desorption of the reactant. The optimal catalyst would therefore have the perfect balance in the interaction with the adsorbate. It has been shown that the minimum theoretical overpotential for oxides is between 0.3 V and 0.4 V [1] according to the widely used mechanism (a four proton-coupled electron-transfer process) for the OER. On the other side, various alternative mechanism has been proposed for the OER, which can, in principle, reduce this overpotential. The mechanisms however depend on many factors, including the class of materials under study and the reaction environment [2–4].

Finding a stable catalyst, with light harvesting properties, for OER is one of the main challenges for photoelectrochemical cells (PECs). Photoferroic materials are an emerging class of materials, which have both photovoltaic and ferroelectric properties. Their spontaneous polarization enhances the photovoltaic effect and helps charge separation [5]. Moreover, their polarization can be switched leading to an enhanced water splitting reaction [6,7]. This is due to the impact of having a catalytic dynamic surface, which is tuned to better fit the reaction and overcomes limitation Sabatier's principle [8].

$InSnO_2N$ is a promising candidate for photocatalysis. It has a band gap in the visible range (1.61 eV) showing a high light absorption. Moreover, it exhibits spontaneous polarization, switchable with an external electric field, and good catalytic properties for OER. The overpotential for OER has been calculated to be 0.77 V on the positively polarized structure, and 0.58 V on negatively polarized one. When switching polarization direction of the $InSnO_2N$ surface during OER process, this value is theoretically predicted to decrease to 0.20 V, which overcomes the limitation of Sabatier's principle [9].

* Corresponding authors at: School of Materials Science and Engineering, Hefei University of Technology, Hefei, Anhui 230009, PR China (Z. Lan); Department of Energy Conversion and Storage, Technical University of Denmark, Anker Engelundsvej 411, DK-2800 Kgs. Lyngby, Denmark (I.E. Castelli).

E-mail addresses: zhenyunlan@hfut.edu.cn (Z. Lan), ivca@dtu.dk (I.E. Castelli).

https://doi.org/10.1016/j.jcat.2022.07.021
0021-9517/

The OER performance can be enhanced by changing the surface structure and electronic properties of the material. Applying a strain to the material can impact the adsorption and desorption strength of the molecules with the surface, leading in some cases to a more efficient reaction [10]. Different types of strain can be applied on a material, depending on its direction (tensile or compressive) and its axis (uniaxial, biaxial, etc.). In epitaxial $LaNiO_3$, compressive strain enhances OER, due to a shift of the Fermi level [11]. Similarly, tensile strain on Pt doped Ti_2CF_2 has led to a lower overpotential for the reaction [12]. A 1 % uniaxial tensile strain on $BaTaO_2N$, under operational conditions, was calculated to reduce the overpotential to 0.37 V, approaching the theoretical minimum for oxides [13].

In this work, biaxial strain is applied to $InSnO_2N$ to analyze the changes in the OER performance to strain. Firstly, the response on its bulk structure was studied, showing that the material is stable and remains ferroelectric under different strains. Then, the impact on OER performance on the two oppositely polarizes structures was analyzed. The results showed that −2.5 % compressive strain and 2.3 % tensile strain on the positively and negatively polarized slabs, respectively, lead to the best performance, with an overpotential of 0.45 V and 0.40 V. Based on this, the impact of dynamic strain, polarization switching, and their combination is also studied. While dynamic strain decreases only slightly the overpotential (to 0.43 V and 0.35 V), polarization switching on a strained structure, both with a static strain and tunable one, leads to a drastic decrease of it. Switching polarization on a structure with −0.5 % strain has led to an overpotential of 0.16 V. When combined with a tunable strain, this is lowered to 0.05 V.

2. Method

In this work, the Vienna Ab Initio Simulation Package (VASP) was used [14,15]. The Perdew-Burke-Ernzerhof (PBE) functional in the framework of the generalized gradient approximation is employed to describe exchange and correlation effects [16]. The frozen core electrons and nuclei of each atom are represented using the projector augmented waves potentials (PAW) [17]. In (5 s, 5d, and 5p), Sn(5 s, 4d and 5p), O(2 s and 2p) and N(3 s and 3p) are defined as valence electrons, with 520 eV plane wave cut-off energy. Artificial interaction between periodic images is avoided by adding a 20 Å vacuum thickness. Dipole correction is also included [18]. Van der Waals interactions are included by adding the Grimme's D3-correction [19]. The atomic positions were relaxed until the forces on the atoms were below 0.02 eV/Å.

From each simulation, the total energy was found and then used to calculate the free energy change. The vibrational frequencies were also calculated, to then compute the zero-point energy (ZPE). The Born effective charges are found with the density functional perturbation theory (DFPT) [20] and used to calculate the polarization following the Born effective charge method [21].

For the bulk structure (30 atoms), a $6 \times 6 \times 3$ Γ-centered Monkhorst Pack k-point mesh was used. For the slab models (66 atoms), a $6 \times 6 \times 1$ mesh for slab models was used [22]. The lattice parameters without any strain applied are a = b = 6.16 Å and c = 12.24 Å.

OER is considered at standard conditions (T = 298 K, p = 1 bar, pH = 0 and U = 0) and the mechanism adopted is a commonly used one, consisting of four Proton-Coupled Electron Transfer (PCET) steps [1,23]:

$$A: * + H_2O \rightarrow OH^* + H^+ + e^- \quad (1)$$

$$B: OH^* \rightarrow O^* + H^+ + e^- \quad (2)$$

$$C: O^* + H_2O \rightarrow OOH^* + H^+ + e^- \quad (3)$$

$$D: OOH^* \rightarrow * + O_2 + H^+ + e^- \quad (4)$$

where the symbol * represents a surface reaction site and O*, OH* and OOH* are intermediates.

The entire process has an energy change of 4.92 eV. (i.e. 1.23 V for per proton–electron pair transfer). Gibbs free energy change (ΔG) of each charge transfer step is calculated by:

$$\Delta G(U, pH, T) = \Delta E + \Delta ZPE - T\Delta S + \Delta G_U + \Delta G_{pH} \quad (5)$$

where, ΔE is the reaction energy from the DFT total energies. ΔZPE and ΔS are zero-point energy difference and entropy difference, respectively. ΔG_U and ΔG_{pH} are the free energy change due to electrode potential U and pH, respectively. Since the free energy change ΔG of each charge transfer step is affected by the same value of ΔG_{pH} at pH ≠ 0 and the theoretical overpotential, η, is defined to be the reaction potential minus the equilibrium potential for water oxidization, the theoretical overpotential η is independent of pH. The volcano plot is constructed from the values of (- η) and (ΔG_{O^*} - ΔG_{OH^*}). All data are stored and freely available in the DTU Data Repository [24].

3. Results and discussion

The impact of biaxial strain on $InSnO_2N$ was first analyzed on its bulk structure to assess possible changes in intrinsic polarization or other impacts on the stability of the material. A strain ranging from −3% to + 3 % was applied to both the centro-symmetric ($P3c1$ space group, Fig. 1.a) and polar structures ($P6_3cm$ space group, Fig. 1.b and 1.c for the positively and negatively polarized surface, respectively).

The polar structure was relaxed during the optimization, keeping the a and b lattice parameters constrained. During structure optimization, we note that the c-parameter decreases/increases linearly with the strain accommodating the changes in the ab-plane. The non-polarized structure was not relaxed to prevent it from going through a phase transition to the polar configuration. The polar structure is always more stable than the non-polar one. The difference between the energy of the two structures increases with the strain, as shown in Fig. 2.b. As illustrated in Fig. 2.a, the polarization increases linearly with the strain: the atom gets further away from the centrosymmetric position as the lattice parameters are extended. The change in polarization, between −3% and + 3 %, is 1.393 μC/m^2, with a 13 % change. The ferroelectric properties of $InSnO_2N$ are therefore always maintained and only slightly affected by strain.

The energy difference is used to calculate the energy barrier for switching the polarization direction when a strain is applied, illustrated in Fig. 2.b. With −2% strain, the energy barrier is 4.02 meV/atom, with 2 % strain it is 11.46 meV/atom, against 5.50 meV/atom without any strain [9]. It can be noted that the energy barrier does not change linearly with the strain: as the strain becomes larger (tensile), its impact on the barrier amplifies, increasing notably its value, while for compressive strains it seems to reach a plateau after 1 %. Switching polarization can lead to even lower overpotentials, and its energy cost can be compared to the reduction in the energy requirement as indicator of the reaction efficiency [8].

The impact of strain was then analyzed on the slab structure. This is composed of nine layers: the bottom four layers were kept fixed during the simulation, while the five upper ones were relaxed, as shown Fig. 3.a.

The preferred adsorption sites are found to be constant over polarization and different strains. The reaction starts on the clean surface, where OH∗ is adsorbed on top of Sn (step 1, Fig. 3.b). OH* is then deprotonated into O∗, which is adsorbed on the hollow site (step 2, Fig. 3.b). OOH ∗ is the formed and adsorbed on top of

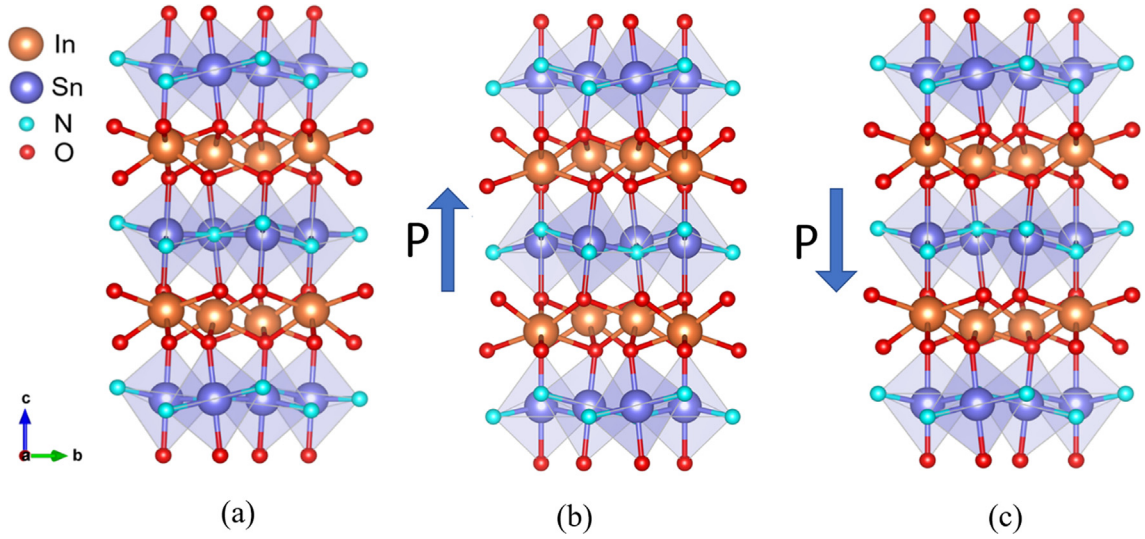

Fig. 1. Unit cell of $InSnO_2N$. The arrow indicates the direction of polarization. (a) Centrosymmetric structure, space group *P*3*c*1 (b) Positively polarized structure, space group $P6_3cm$ (c) Negatively polarized structure, space group $P6_3cm$.

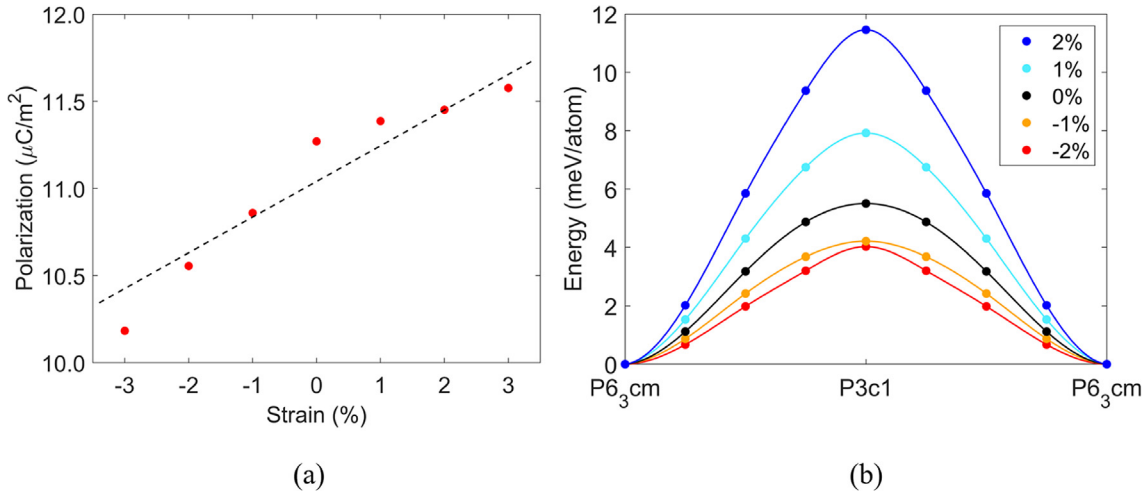

Fig. 2. (a) Polarization in function of the strain, with the strain ranging from −3% to 3% (b) Energy barrier to switch polarization, passing through the *P*3*c*1 phase, for compressive and tensile strains ranging from −2% to 2%.

Sn (step 3, Fig. 3.b). Finally, OOH* is deprotonated with the formation of O_2 (step 4, Fig. 3.b), and the reaction can start over.

Fig. 4.a and b show the impact of biaxial strain on OER for the two oppositely polarized slabs. For both polarizations, a more compressive strain leads to a stronger adsorption. Nevertheless, the strain resulting in an optimal OER performance is opposite: for the positively polarized structure it is a compressive strain, while for the negatively polarized structure, it is a tensile strain. The change in the slope and position of the top could be related to the changes in the polarization, which breaks the scaling relations.

On the positively polarized slab, the overpotential reaches a value 0.45 V when a compressive strain of −2.5 % is applied, 0.32 V lower than the overpotential on the unstrained structure (0.77 V). The potential determining step in the OER reaction is the formation of O_2 from OOH∗ with an energy requirement of 1.68 eV, as illustrated in Fig. 4.c. For the negatively polarized structure, a tensile strain of 2.3 % decreases the overpotential from 0.58 V (unstrained structure) to 0.40 V. The potential determining step is the formation of O∗ from OH∗ with an energy requirement of 1.63 eV, as shown in Fig. 4.d.

The electronic structure of the surface layers was investigated with the layer-resolved partial density of states (PDOS). As it can be seen in Fig. 5, with more compressive strains, the Fermi level increases in energy, meaning that more electrons are available on the surface. Compressing and dilating the structure causes a displacement of the electrons in the opposite direction. When the structure is compressed, they are pushed up to the surface layers, if it is extended, they are pushed down to the deeper layers.

This can explain the catalytic behaviour of the material under different strains. More electrons on the surface lead to a weaker bond between the negatively charged adsorbate and the surface. As, for the same strain, the positively polarized slab has a higher Fermi level than the negatively polarized one, the potential determining steps of the reaction are different, and the optimal strain is opposite between the two structures.

The optimal strain, −2.5 %, on the positively polarized structure has a Fermi level higher than the non-strained case (Fig. 5.a). More

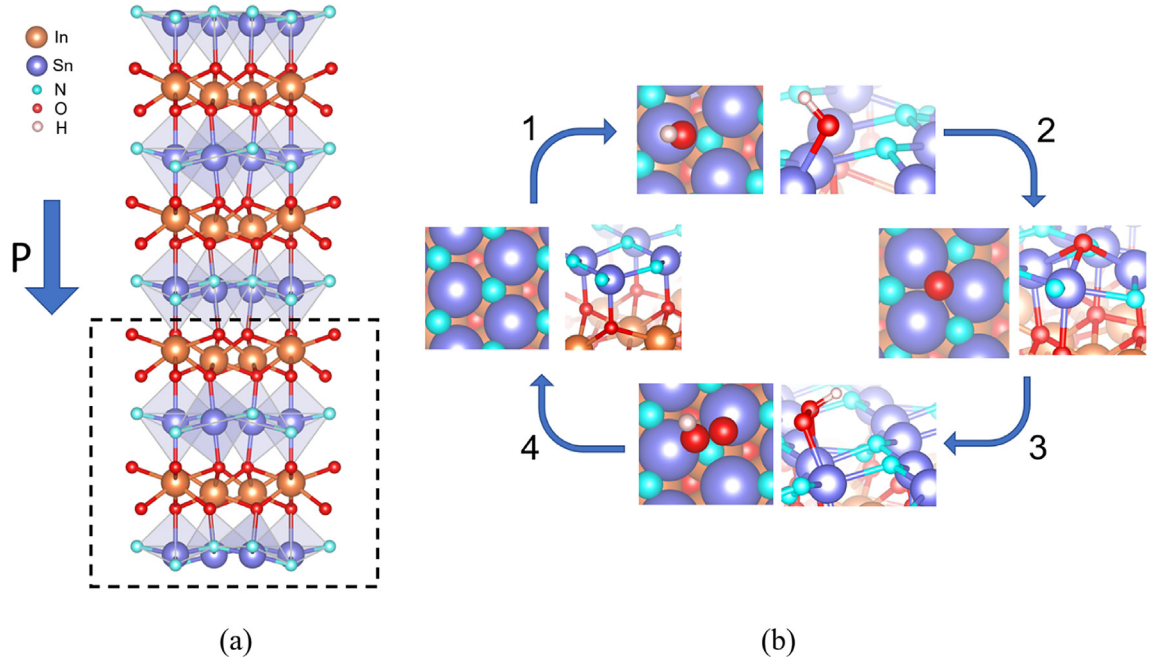

Fig. 3. Slab structures and adsorption sites. (a) Negatively polarized slab structure. The arrow indicates the direction of polarization, the atoms in the dashed rectangle are fixed during the optimization. (b) OER steps and preferred adsorption sites on the negatively polarized slab, top view, and lateral view. The numbers indicate the reaction step. On the positively polarized case, the adsorption sites are the same but with slightly different orientation of the molecules.

electrons are available and the bonding with the adsorbate is weaker. A larger compressive strain would lead to an even higher Fermi level and an interaction that would be too weak.

Oppositely, the optimal strain, 2.3 %, on the negatively polarized structure has lower Fermi level than the non-strained one (Fig. 5. b). The electrons are displaced to deeper layers and the bonding with the adsorbate is stronger. Increasing the strain further would lead to a too strong interaction.

Applying biaxial strain to $InSnO_2N$ therefore induces a change of its electronic structure, which in turn affects its catalytic properties. The opposite response to tensile and compressive strains on the two polarized structures leads to a different potential determining step for the two surfaces. Thus, we can lower the overpotential by changing strain or switching polarization direction.

3.1. Dynamic strain

On the positively polarized structure, the strain can be tuned between step 2 and 3 and then between step 3 and 4, as illustrated in Fig. 6. For all large compressive strains, the third step still has a relatively high energy requirement and would become the potential determining step when a dynamic strain is applied. The lowest value that can be reached is 0.43 V, with either −4% or −3% strain tuned with any strain higher than −2.5 %. This is only 0.02 V lower than the optimal static strain, and a large strain would still need to be applied. The change in strain would lead to a transfer of electrons from the bottom layers to the surface ones, and then back. On the negatively polarized structure, the strain can be changed between step 1 and 2, and then between step 2 and 3, as in Fig. 5.b. The potential determining step now becomes the second one, and the overpotential can reach a minimum of 0.35 V with 3 % strain combined with any strain lower than 2.3 %. This is 0.05 V lower than when applying a static strain. The electrons are first displaced from the surface layers to the bottom ones and then back. In both cases, applying a dynamic strain is not convenient as the overpotential does not decrease significantly: a large strain would still be needed, it would be hard to control its value and the material can break easily.

3.2. Polarization switching and static strain

The different interaction between the adsorbate and the surface on the two oppositely polarized structures can be exploited by switching the polarization. It has already shown a decrease of the overpotential to 0.20 V on the non-strained structure [9]. Thus, polarization switching can be applied for strains between −0.5 % and 2 %, where the potential determining step on the two opposite polarization is a different one.

The positively polarized structures are limited by the formation of OOH∗ from O∗ while the negatively polarized ones are limited by the formation of O∗ from OH*. Thus, we should switch the polarization from negative to positive between step 1 and 2 and then again from positive to negative between step 2 and 3, as illustrated in Fig. 7.

The reaction starts with the deprotonation of H_2O and adsorption of OH on the negatively polarized structure. Here the polarization is switched and the OH molecule is adsorbed on the positively polarized surface, where it is deprotonated into O. The polarization is then be switched back and OOH is formed on the negatively polarized surface. Finally, O_2 is formed with the deprotonation of OOH. The overpotential always reaches a lower level compared to the ideal case of 0.37 V, but only with −0.5 % strain the result obtained is better than without any strain. The overpotential is now 0.16 V and the potential determining step is the formation of O∗ from OH∗, as illustrated in Fig. 7. In all the other cases, the third step on the negatively polarized slab becomes the potential determining one.

3.3. Polarization switching and dynamic strain

The overpotential reached before can be further lowered by matching the polarization switch with a tuning of the strain. The

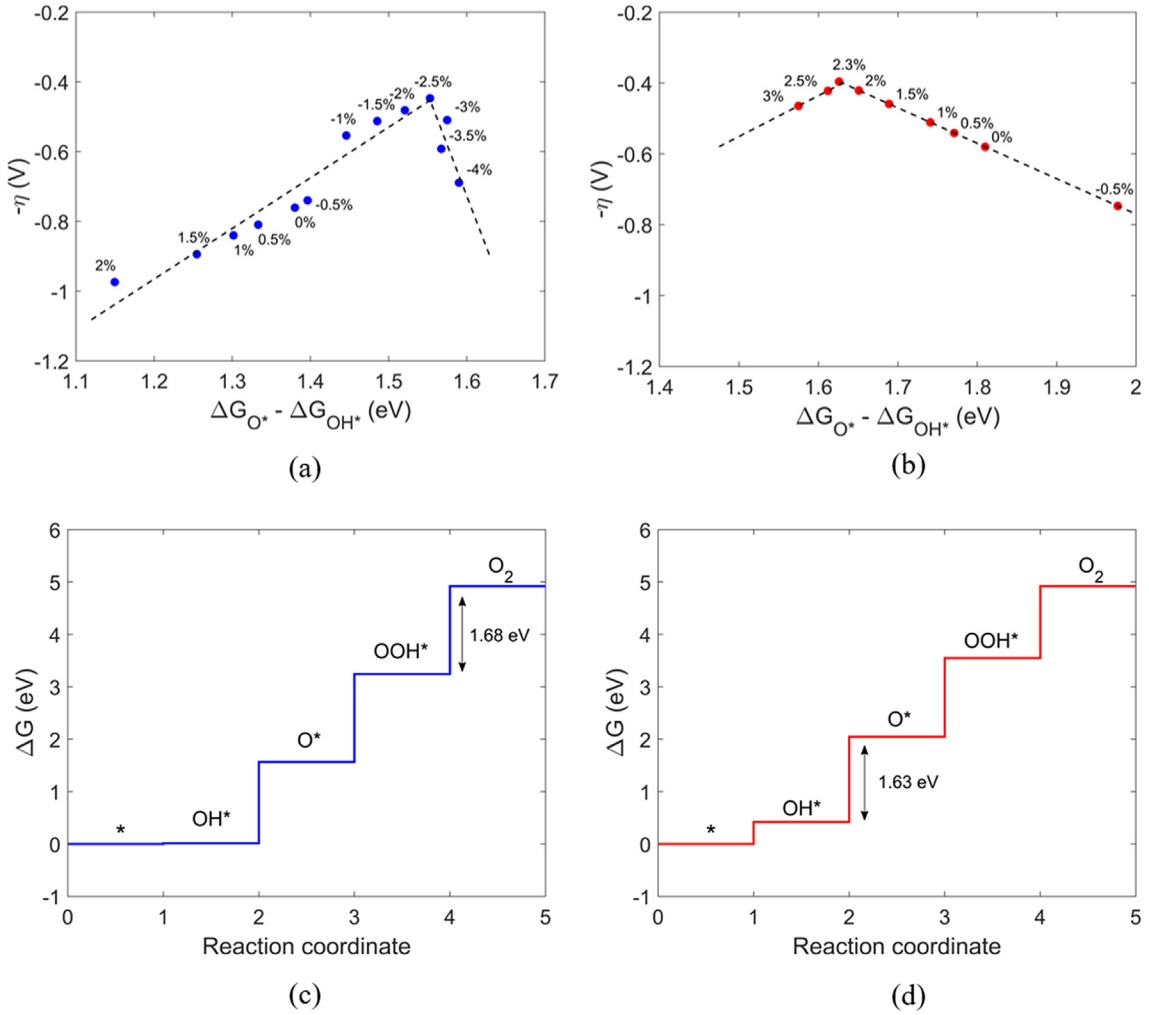

Fig. 4. Volcano plots of the free energy difference $\Delta G_{O^*} - \Delta G_{OH^*}$ and the overpotential η, Gibbs free energy diagrams of the optimal cases. The potential determining step is indicated with the double arrow and the corresponding energy requirement (a) Volcano plot for the positively polarized slab (b) Volcano plot for the negatively polarized slab (c) Gibbs free energy diagram for the positively polarized slab with −2.5% strain. The potential determining step is the formation of O_2. (d) Gibbs free energy diagram for the negatively polarized slab with 2.3% strain. The potential determining step is the formation of O.

structures should be combined such that the potential determining step of one is as low as possible in the other.

The positively polarized slab with 2 % strain has the lowest second step while the negatively polarized slab with −0.5 % strain has the lowest requirement in the third step. Thus, the polarization and the strain can be switched between step 1 and 2 from the positively polarized slab with 2 % strain to the negatively polarized one with −0.5 % strain, and then back between step 2 and 3. The potential determining step is the formation of O_2 from OOH∗, with an energy requirement of 1.28 eV, as illustrated in Fig. 8. This leads to a drastic decrease of the overpotential, which now has a value of 0.05 V.

The low energy requirement reached with this method highlights the potential of having a dynamic surface of the catalyst. The surface structure can in fact be tuned almost optimally to fit the reaction and adsorbate requirements.

Between the methods analysed, polarization switching with a −0.5 % static strain is the most promising one. Switching polarization has been experimentally proved on h-$ErMnO_3$ with a frequency range from 0.1 to 1000 Hz [25], which covers the optimal resonant range for representative catalytic reactions like formic acid oxidation [26] and the practical implementation of switched $InSnO_2N$ ferroelectric photocatalysts should be allowed. On the other side, strain tunability involves much longer time scales. The strain can be applied in different ways, from using an external mechanical stress to use heterostructures composed of $InSnO_2N$ on piezoelectric or electrostrictive materials. On the other hand, if only a static or dynamic strain is applied, then it would need to be large and this can break the material, compromising the whole reaction.

Employing a highly dynamic surface, where both strain and polarization change, would be incredibly challenging although promising to further reduce the reaction overpotentials. A dynamic strain can be implemented by controlling the physical alteration of the substrate. This has been successfully proved experimentally with intercalation of Li ions on $LiCoO_2$, leading to a 3–5 % tuneable strain in the Pt overlayer [10]. A mechanical deformation of the substrate, specifically poly(methyl methacrylate) diaphragm, has also led to a tunable strain on the Tungsten Carbide overlayer [27].

However, the strain is hard to properly control, and the material can easily break because of the continuous variation in its lattice parameters and structure geometry [8]. Moreover, for $InSnO_2N$, the direction of its polarization should change synchronously with the strain, heavily increasing the size of the challenge. The changes in strain and polarization need also to be repeated cyclically to run the reaction. The material should be elastic enough to support the

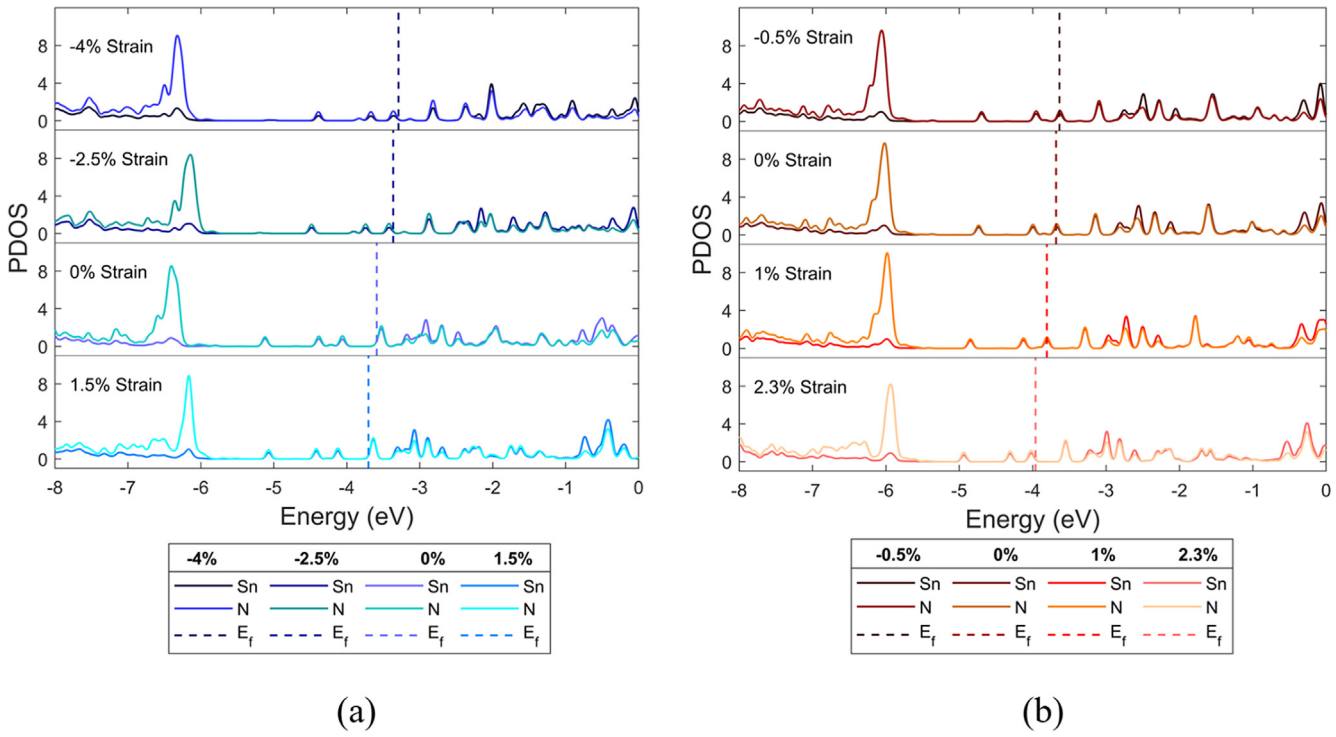

Fig. 5. Partial density of states for the first layer of the slab structure with different strains. The dashed lines represent the Fermi levels. (a) Positive polarized slab with −4%, −2.5%, 0% and 1.5% strain (b) Negative polarized slab, with −0.5%, 0%, 1% and 2.3% strain.

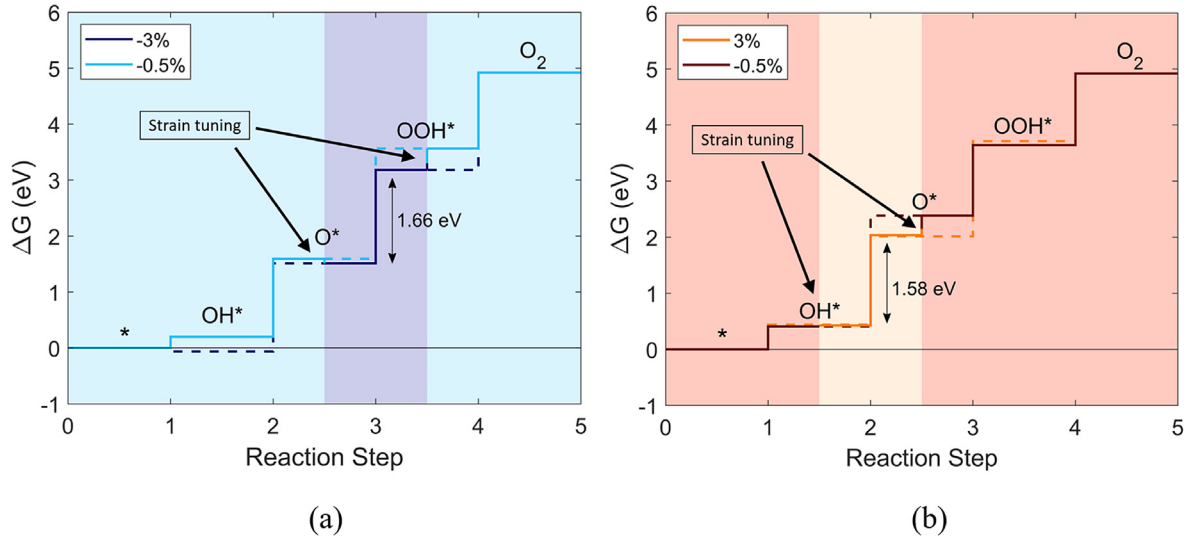

Fig. 6. Gibbs free diagrams for $InSnO_2N$ with a dynamic strain. The continuous lines illustrate the reaction path taken. The dashed lines follow the path without dynamic strain. The potential determining step is indicated with the double arrow and the corresponding energy requirement. (a) Positively polarized slab with strain tuned between −0.5 % and −3% (b) Negatively polarized slab with strain tuned between −0.5 % and 2.5 %.

change in the structure without any repercussions on its catalytic activity. Also computationally, it was necessary to apply the strain step by step, as compressing or extending too much the material at once causes a displacement of Nitrogen atoms of the internal layers.

Studying more in detail the chemistry of the reaction on a dynamic surface is hard from a computational point of view. More variables are needed to describe the system, increasing the time for the simulations. Moreover, the model might not be able to evaluate the real case properly, as the understanding of the impact of external manipulation on the surface properties is still limited [8]. An investigation of the $InSnO_2N$ surface under different operational conditions for the catalytic activity is a natural extension of the present work.

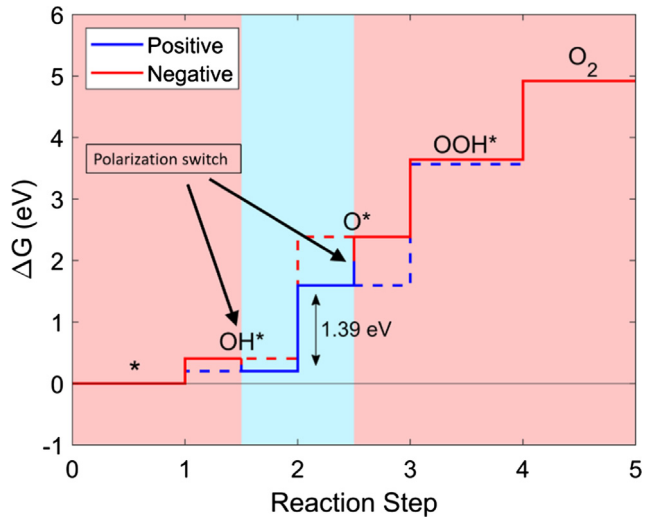

Fig. 7. Gibbs free energy diagram of OER with −0.5% strain and polarization switching, between step 1 and 2, and step 2 and 3. The potential determining step is indicated with the double arrow and the corresponding energy requirement.

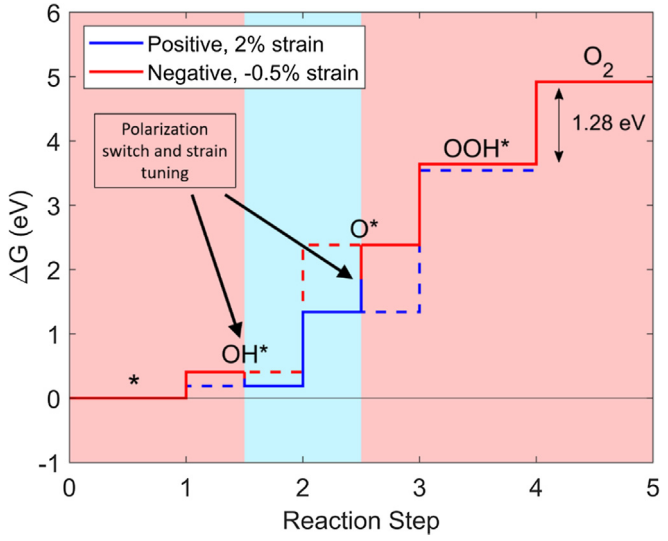

Fig. 8. Gibbs free energy diagram for the reaction with dynamic strain and polarization switching between step 1 and 2, and step 2 and 3. The potential determining step is indicated with the double arrow and the corresponding energy requirement.

4. Conclusion

In this work, the impact of biaxial strain on the catalytic properties of $InSnO_2N$ for the oxygen evolution reaction was investigated with DFT. For the positively polarized structure, a compressive strain of −2.5 % has reduced the overpotential from 0.77 V to 0.45 V. For the negatively polarized structure, the overpotential decreased from 0.58 V to 0.40 V with a tensile strain of 2.3 %. These values are close to the ideal value (0.37 V). The opposite impact of the strain on the two polarizations was then related to the partial density of states and the displacement of electrons. A compressive strain leads to a movement of electrons towards the surface layers, and a higher Fermi level, while a tensile one towards the deeper layers, with a lower Fermi level.

Applying a dynamic strain leads to an overpotential of 0.43 V and 0.35 V for the positively and negatively polarized structures respectively. If the polarization is switched while a compressive strain of −0.5 % is applied, the overpotential reaches a value of 0.16 V. This is below the result achieved on the non-strained structure (0.20 V) and far lower than the ideal case for oxynitrides (0.37 V). The reduction of the energy requirement outweights the energy cost of applying a small strain and switching the polarization. Combining a dynamic strain with polarization switching decreases the overpotential to 0.05 V.

The strategy of combining dynamic strain and switching polarization can be applied to other materials to improve their catalytic performance. If the material is elastic and not at high risk of breaking, then a dynamic control of its surface can drastically improve the reaction, since the structure can be tuned to better fit the adsorbates. For ferroelectric materials, polarization switching, possibly combined with strain engineering, is confirmed to be a practical method to enhance the OER performance.

Declaration of Competing Interest

The authors declare that they have no known competing financial interests or personal relationships that could have appeared to influence the work reported in this paper.

References

[1] I.C. Man, H.Y. Su, F. Calle-Vallejo, H.A. Hansen, J.I. Martínez, N.G. Inoglu, J. Kitchin, T.F. Jaramillo, J.K. Nørskov, J. Rossmeisl, Universality in oxygen evolution electrocatalysis on oxide surfaces, ChemCatChem 3 (2011) 1159–1165, https://doi.org/10.1002/cctc.201000397.
[2] R. Frydendal, M. Busch, N.B. Halck, E.A. Paoli, P. Krtil, I. Chorkendorff, J. Rossmeisl, Enhancing activity for the oxygen evolution reaction: the beneficial interaction of gold with manganese and cobalt oxides, ChemCatChem 7 (2015) 149–154, https://doi.org/10.1002/cctc.201402756.
[3] M. Busch, N.B. Halck, U.I. Kramm, S. Siahrostami, P. Krtil, J. Rossmeisl, Beyond the top of the volcano? – A unified approach to electrocatalytic oxygen reduction and oxygen evolution, Nano Energy 29 (2016) 126–135, https://doi.org/10.1016/j.nanoen.2016.04.011.
[4] L. Bai, S. Lee, X. Hu, Spectroscopic and electrokinetic evidence for a bifunctional mechanism of the oxygen evolution reaction**, Angew. Chem. Int. Ed. 60 (2021) 3095–3103, https://doi.org/10.1002/anie.202011388.
[5] L. Li, P.A. Salvador, G.S. Rohrer, Photocatalysts with internal electric fields, Nanoscale. 6 (2014) 24–42, https://doi.org/10.1039/c3nr03998f.
[6] J.H. Lee, A. Selloni, TiO_2 /ferroelectric heterostructures as dynamic polarization-promoted catalysts for photochemical and electrochemical oxidation of water, Phys. Rev. Lett. 112 (2014) 196102, https://doi.org/10.1103/PhysRevLett.112.196102.
[7] I.E. Castelli, T. Olsen, Y. Chen, Towards photoferroic materials by design: Recent progress and perspectives, J. Phys. Energy. 2 (1) (2020) 011001, https://doi.org/10.1088/2515-7655/ab428c.
[8] M. Shetty, A. Walton, S.R. Gathmann, M.A. Ardagh, J. Gopeesingh, J. Resasco, T. Birol, Q. Zhang, M. Tsapatsis, D.G. Vlachos, P. Christopher, C.D. Frisbie, O.A. Abdelrahman, P.J. Dauenhauer, The catalytic mechanics of dynamic surfaces: stimulating methods for promoting catalytic resonance, ACS Catal. 10 (2020) 12666–12695, https://doi.org/10.1021/acscatal.0c03336.
[9] Z. Lan, D.R. Småbråten, C. Xiao, T. Vegge, U. Aschauer, I.E. Castelli, Enhancing oxygen evolution reaction activity by using switchable polarization in ferroelectric InSnO2N, ACS Catal. 11 (2021) 12692–12700, https://doi.org/10.1021/acscatal.1c03737.
[10] J. Hwang, Z. Feng, N. Charles, X.R. Wang, D. Lee, K.A. Stoerzinger, S. Muy, R.R. Rao, D. Lee, R. Jacobs, D. Morgan, Y. Shao-Horn, Tuning perovskite oxides by strain: electronic structure, properties, and functions in (electro)catalysis and ferroelectricity, Mater. Today 31 (2019) 100–118, https://doi.org/10.1016/j.mattod.2019.03.014.
[11] J.R. Petrie, V.R. Cooper, J.W. Freeland, T.L. Meyer, Z. Zhang, D.A. Lutterman, H.N. Lee, enhanced bifunctional oxygen catalysis in strained LaNiO3 perovskites, J. Am. Chem. Soc. 138 (2016) 2488–2491, https://doi.org/10.1021/jacs.5b11713.
[12] N. Ma, N. Li, T. Wang, X. Ma, J. Fan, Strain engineering in the oxygen reduction reaction and oxygen evolution reaction catalyzed by Pt-doped Ti_2 CF_2, J. Mater. Chem. A 10 (2022) 1390–1401, https://doi.org/10.1039/D1TA07349D.
[13] Z. Lan, T. Vegge, I.E. Castelli, Theoretical insight on anion ordering, strain, and doping engineering of the oxygen evolution reaction in BaTaO2N, Chem. Mater. 33 (2021) 3297–3303, https://doi.org/10.1021/acs.chemmater.1c00370.
[14] G. Kresse, J. Furthmüller, Efficient Iterative Schemes for Ab-initio Total-energy Calculations using a Plane-wave Basis Set, Phys. Rev. B 54 (1996) 11169, https://doi.org/10.1103/PhysRevB.54.11169.
[15] G. Kresse, J. Hafner, Ab-initio Molecular Dynamics for Liquid Metals, Phys. Rev. B 47 (1993) 558, https://doi.org/10.1103/PhysRevB.47.558.
[16] J.P. Perdew, K. Burke, M. Ernzerhof, Generalized Gradient Approximation Made Simple, Phys. Rev. Lett. 77 (1996) 3865, https://doi.org/10.1103/PhysRevLett.77.3865.

[17] G. Kresse, D. Joubert, From Ultrasoft Pseudopotentials to the Projector Augmented-wave Method, Phys. Rev. B 59 (1999) 1758, doi:10.1103/PhysRevB.59.1758.
[18] L. Bengtsson, Dipole Correction for Surface Supercell Calculations, Phys. Rev. B 59 (1999) 12301, doi:10.1103/PhysRevB.59.12301.
[19] S. Grimme, J. Antony, S. Ehrlich, H. Krieg, A Consistent and Accurate Ab-initio Parametrization of Density Functional Dispersion Correction (DFT-D) for the 94 Elements H-Pu, J. Chem. Phys. 132 (15) (2010) 154104.
[20] S. Baroni, P. Giannozzi, A. Testa, Green's-Function Approach to Linear Response in Solids, Phys. Rev. Lett. 58 (1997) 1861, doi:0.1103/PhysRevLett.58.1861.
[21] J.B. Neaton, C. Ederer, U. V. Waghmare, N.A. Spaldin, K.M. Rabe, First-principles study of spontaneous polarization in multiferroic $BiFeO_3$, Phys. Rev. B (2005) 71, doi:10.1103/PhysRevB.71.014113.
[22] H.J. Monkhorst, J.D. Pack, Special Points for Brillonin-zone Integrations, Phys. Rev. B 13 (1976) 5188, doi:10.1103/PhysRevB.13.5188.
[23] Y.F. Li, First-principles simulations for morphology and structural evolutions of catalysts in oxygen evolution reaction, ChemSusChem 12 (2019) 1846–1857, https://doi.org/10.1002/cssc.201802525.
[24] Dataset for Dynamic Strain and Switchable Polarization: a Pathway to Enhance the Oxygen Evolution Reaction on InSnO 2N; DTU Data Repository, doi:10.11583/DTU.20209391, 2022.
[25] A. Ruff, Z. Li, A. Loidl, J. Schaab, M. Fiebig, A. Cano, Z. Yan, E. Bourret, J. Glaum, D. Meier, S. Krohns, Frequency Dependent Polarisation Switching in h-$ErMnO_3$, Appl. Phys. Lett. 112 (18) (2018) 182908, https://doi.org/10.1063/1.5026732.
[26] J. Gopeesingh, M.A. Ardagh, M. Shetty, S.T. Burke, P.J. Dauenhauer, O.A. Abdelrahman, Resonance-promoted formic acid oxidation via dynamic electrocatalytic modulation, ACS Catal. 10 (2020) 9932–9942, https://doi.org/10.1021/acscatal.0c02201.
[27] K. Yan, S.K. Kim, A. Khorshidi, P.R. Guduru, A.A. Peterson, High elastic strain directly tunes the hydrogen evolution reaction on tungsten carbide, J. Phys. Chem. C. 121 (2017) 6177–6183, https://doi.org/10.1021/acs.jpcc.7b00281.